ACOUSTIC EMISSION SIGNATURE ANALYSIS ON ROLLING ELEMENT BEARINGS DUE TO LOCALIZED DEFECTS

Ratnam Chanamala[1], Nerella Mary Jasmin[1], Rao Vana Vital[2], Rao K. Venkata[3]

[1]Andhra University College of Engineering (A), Department of mechanical engineering
Visakhapatanam, Andhra Pradesh 530003, India
[2]AGM, Shops & Foundry Dept., Visakhapatnam Steel Plant
Visakhapatnam, Andhra Pradesh 530031, India
[3]Vignan's Foundation for Science, Technology and Research
Mechanical Engineering Department, Guntur, Andhra Pradesh 522213, India

Corresponding author: Mary Jasmin Nerella, jasminmary2@gmail.com

Abstract: The interaction of surface asperities and impingement of rolling element of bearing over the defective races of rolling element bearings generate Acoustic Emissions (AEs). Significant progress in the capabilities of acoustic instrumentation, together with signal processing techniques, made possible to extract useful diagnostic information from acoustic signals. The main advantage of AE is that it offers high Signal to Noise Ratio (SNR), which is required for the precise detection of faults. Rotating speed, radial load and size of localized defect are the most influenced operating parameters on AE amplitude. A bearing test-rig is designed and established to study the various defect sizes on outer race of rolling element bearings. AE signal generated from artificial line defects in rolling element bearings (REBs) are investigated. The AE signal was transformed through Fast Fourier Transform (FFT) AE laboratory software, which is supplied by AE instrument. Even though there were many signatures of AE signals that can be used such as amplitude, duration, counts and signal energy. AE instrument with amplitude is used in this study, which allows for the measuring of amplitude in the signal. Experiments are performed using N312 REBs and results have been presented. Experimental data is analyzed using response surface methodology (RSM) to identify the significant parameters on AE amplitude. Here, predictive model like RSM is used to predict and optimize AE amplitude in dB level.

Key words: fault diagnosis, rolling element bearings, response surface methodology, analysis of variance.

1. INTRODUCTION

Bearings are mainly used in an extensive variety of rotating machinery from small hand-held devices to heavy duty industrial systems. The common source of bearing damage is mainly due to severe working conditions, high load and operating speed. Vibration signature analysis is the most commonly used fault-detection technique employed in rotor bearing systems. The vibration signal is not sensitive to the incipient defects in the bearings; sometimes the defect frequencies are not observable into FFT spectrum, because the impulses generated by the defects are masked or distorted by the noise generated by other parts of the equipment. To overcome this problem, advanced signal processing techniques are implemented by many researchers to detect bearing local faults (Bouchra Abou El Anouar, 2017). AE is receiving an extreme attention as a complementary method for condition monitoring of bearings being very sensitive to incipient defects (Jaeyoung, 2017; Ked douche et al., 2014). REB defects may be categorized as localized defects and distributed defects. Surface roughness, waviness, misaligned races and off-size rolling elements are included in the class of distributed defects (Tandon and Choudhury, 2000). The localized defects include cracks, pits and spalls caused by fatigue on the rolling surfaces (Tandon and Choudhury, 1999). The periodic impacts were occurred at ball-passing frequency (characteristic defect frequencies), which can be estimated from the bearing geometry and the rotational speed. Based on vibration and acoustic signal processing there were several methods have been developed to detect the localized faults in REB (Rao et al., 2015). The interaction of surface asperities and impingement of the balls over the seeded defects on the outer race generates AE signals which are basically the transient elastic waves. During the last few years a significant progress in the capabilities of acoustic instrumentation together with the signal processing techniques had made it possible to extract useful diagnostic information from acoustic signals (Cockerill et al., 2016; Caesarendra et al., 2016; Gu et al., 2011; Al-Obaidi et al., 2012; Nerella et al., 2017; Ked douche et al., 2014). Generally, the vibration accelerometers only pick up signals below a frequency of 20 kHz. Low-frequency related problems, such as rotor unbalance,

misalignment, severe damage in the bearing, rubbing, etc, can be easily diagnosed with vibration analysis. AE sensors can pick up signals between 100 kHz to 1 MHz in frequency, hence low frequency related problems will not interfere with the AE signals generated by the fatigue cracks, incipient damage in bearings, etc. Compared vibration and AE analysis in the identification of bearing defects and reported that the detectability of defects at lower speeds is highest in AE (Rao et al., 2015). Hence, based on these works, AE is considered in the present investigation. Jamadar, et al. (2016) presented a theoretical model for the investigation of the damage severity on the rollers in REBs using theory of dimensional analysis. Effect of various parameters such as spall size, radial load, rotor unbalance, axial load, inner race speed, grease grade, radial clearance, number of rollers etc. on the vibration acceleration amplitude of the bearings were investigated. Experimentally it was observed that the peak vibration acceleration at the characteristic defect frequency increases considerably with increase in the spall sizes. A good agreement between the theoretical and predicted analytical values of the vibration accelerations of the roller damaged bearings was noticed. Farzad Hemmati, et al. (2016) investigated the effect of defect size, operating speed and loading conditions on statistical parameters of AE signals, using design of experiment (DOE) method, to select the most sensitive parameters for diagnosing incipient faults and defect growth on REBs. To estimate the defect size, the Plackett–Burman method was chosen. Experimentally measured defect sizes were compared with their actual values showing a maximum error of 10%. Joao, et al. (2018) contributes to the reduction of vibrations using milling parameters such as cutting speed, feed speed, axial penetration and radial penetration related to the section area. Joao Ribeiro, et al. (2017) study includes an orthogonal array of L9 was used and the analysis of variance (ANOVA), Figure 1, were carried out to identify feed per tooth, cutting speed and radial depth of cut as control factors affecting the surface roughness. The optimal cutting combination was determined by seeking the best surface roughness and SNR ratio, Kankar, et al. (2012), obtained the vibration response analyzed for the un-cracked and cracked rotor with and without defects on bearing components. The defects such as spalls on the outer race, inner race and on the rolling elements were considered. Combined parametric effects had been analyzed to predict the dynamic response of a rotor bearing system. In this paper, the consisted AE amplitudes (dB level) at defect frequencies for a defective bearing with different defects width 0.3mm, 0.5mm, 0.7mm, 0.9mm and 1.1 mm at the outer race under 2 kN and 4 kN loads are recorded. Influenced operating parameters such as defect size, rotating speed and radial load are considered as input parameters. These parameters are tabulated in Table 1.

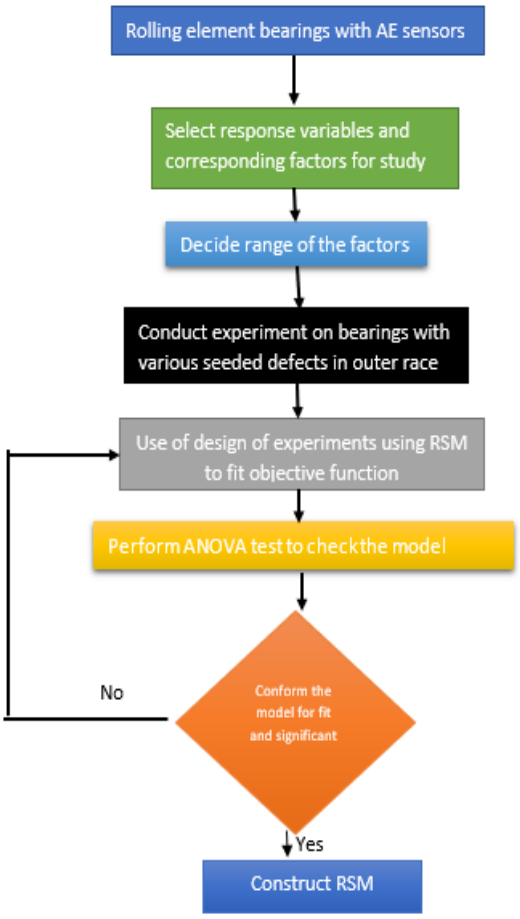

Fig. 1. Flow chart for RSM

Table 1. Parameters for DOE

Designated parameter symbols	Parameters	Minimum level (-)	Maximum level (+)
A	Defect size	0.3 mm	1.1 mm
B	Rotational speed	500 rpm	1500 rpm
C	Radial load	2kN	4kN

2. EXPERIMENTAL WORK

The experimental setup consists of a shaft driven by a different speed range up to 2800 rpm with a 16kN load capacity load and a dismountable bearing test rig which is shown in Figure 2 (a) and (b). On left side the shaft is assembled by V-pulley and on the right side with the test bearings. The shaft is supported on both sides by two concealed deep groove ball bearings with plumber blocks. The 2.2kW power motor placed on a separate base frame to free from vibrations on the test rig and the motor drives the shaft with the V-belt. A N312 roller bearing is mounted in a square type split housing made up of EN 24 steel was used as test bearing housing to enhance the feasibility of introducing faults on the outer race. Moreover, assembly and disassembly of the bearing was accomplished with minimum disruption to the test setup. The load is applied radially on the top of the split housing through hydraulic ram. The AE data

acquisition and sensor used for the bearing fault diagnosis was Holroyd instrument with magnetic mount sensor of model 1030 Mag is used while observing the test run. This instrument works on the acoustic emission principle on operating the high frequency signal. The sensing element is a resonant piezo electric at 100 kHz with integral pre-amplifier of +24dB gain and detecting high frequency stress waves (at approximately 100 kHz) associated with energy loss mechanisms such as friction and impacts that are naturally produced by damaged bearings and other components of machinery. This AE instrument is not sensitive to low frequency activity such as that associated with vibration or audible sound. The bearing parameters are tabulated in Table2.

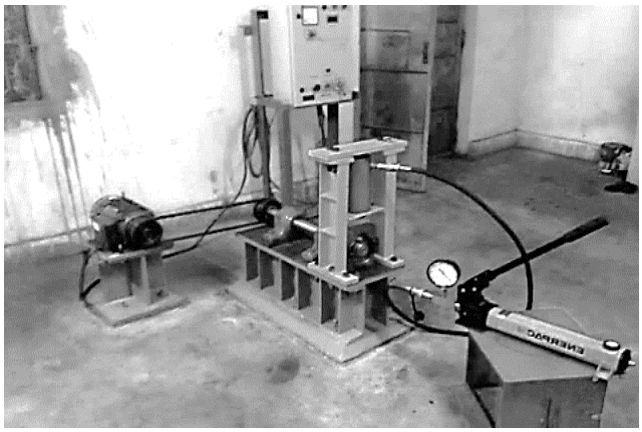

Fig. 2 (a) Experimental test setup

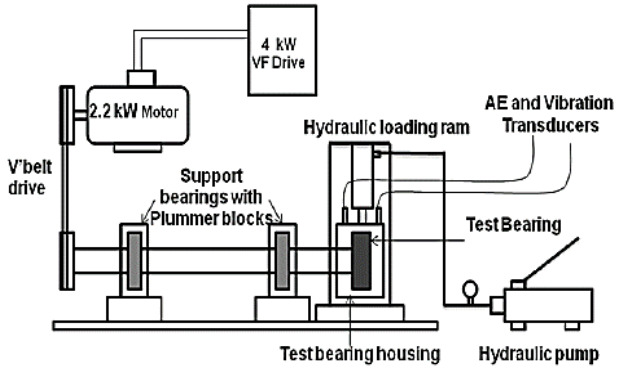

Fig. 2 (b) Setup sketch.

Table 2. Test bearing specifications

Model No.	NTN N312
Rolling element diameter (d)	18mm
Angle in contact (α)	0^0
Width (w)	31mm
Pitch circle diameter (Dp)	96mm
No. of rollers	12
Speed Range	10-3000 rpm
Outer diameter	130mm
Inner diameter	60mm
Mass	1.80Kg
Max load	16kN

3. EXPERIMENTAL PROCEDURE AND STATISTICAL ANALYSIS

The most common signal processing technique is time domain statistical analysis. Signal analysis in time domain has been used to monitor simple machine conditions and faults utilizing statistical parameters. Number of statistical parameters like; RMS amplitude, peak value, crest factor, kurtosis etc. can be derived from the data of time wave signal.
Experimental tests were performed by first making the defects in the appropriate size and geometrical shape. Bearing faults are artificially produced on the outer race by wire cut EDM (Electro Discharge Machining) shown in Figure 3 to control the shape and depth of the faults.

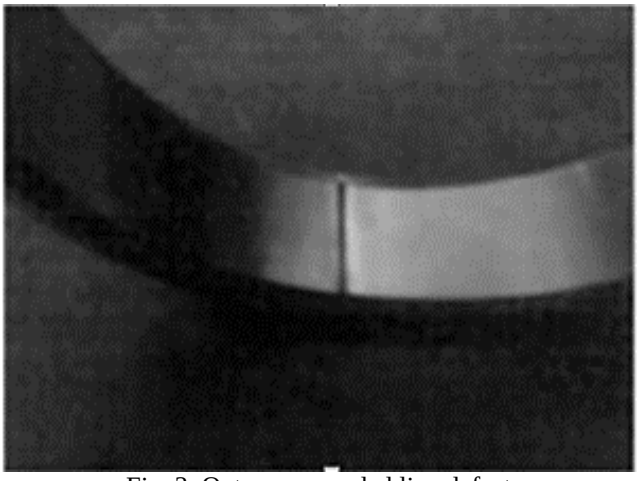

Fig. 3. Outer race seeded line defect

All experiments have been conducted at different rotating speeds from 500 rpm to 1500 rpm and under the loads of 2kN and 4kN. This instrument recorded time wave of 2048 samples data per second to enable a repetition frequency spectrum to be calculated. The AE Lab software provided for the Holroyd instrument is specifically designed to enable AE envelope spectra to be generated and analyzed from time wave. Each AE spectrum covers the frequency range of 0 Hz to 1000 Hz and is representative of a one second period. AE amplitudes (dB level) of statistical measurements were calculated and reported as experimentally measured statistical values.
In the present work, 20 experiments were conducted to predict AE amplitude. The predicted AE amplitude found to be close to experimental values were identified using RSM technique through design expert software. DOE parameters with their minimum and maximum level have been illustrated in Table 2 and set of DOE and result is presented in Table 3.

Table 3. DOE and experimental results of AE amplitude (dB level)

Trail. No.	Design of experiments			AE amplitude (dB)
	Defect size (mm)	Rotational speed (rpm)	Radial load (kN)	
1	0.3	500	2	1.14
2	0.7	700	2	2.71
3	0.7	1100	2	4.58
4	1.1	1500	2	6.87
5	1.1	500	2	3.16
6	1.1	500	4	3.98
7	0.7	1100	4	5.83
8	0.3	1500	2	2.34
9	0.7	1100	4	5.83
10	0.3	500	4	1.13
11	0.7	900	2	3.75
12	0.7	900	2	3.75
13	0.7	900	2	3.75
14	0.7	1100	2	4.58
15	0.7	1300	4	5.31
16	0.7	1300	4	5.31
17	0.5	1300	4	4.21
18	0.5	1100	4	5.84
19	1.1	1500	4	11.8
20	0.3	1500	4	2.34

4. RESULTS AND DISCUSSIONS

N312 bearing is a test roller bearing where outer race can be separated shown in Figure 3 and Figure 4. The main reason for selection of this bearing is easy assemblage and dissembling of outer race. Acoustic emission signal data are recorded and post processed through AE lab software. First, the time versus amplitude data of bearing on its running condition were collected. This instrument recorded the time wave of 2048 samples of data per second to enable a repetition frequency spectrum to be calculated. Each AE envelope spectrum covers the frequency range of 0 Hz to 1000 Hz and in the representative of a one second period. Inside of the outer race surface, defect of different width defects were created with Wire cut EDM. A defect free bearing is assembled in the test bearing house and the test rig was run for minor adjustments. After that, the defect seeded bearing of various sizes were assembled simultaneously in the test bearing house and the defect was positioned at the top. Test runs are conducted at five speeds as N1=500 rpm, N2=700 rpm, N3=900 rpm, N4=1100 rpm, N5=1300 rpm, N6=1500 rpm and at two loads as L1= 4 kN and L2= 2 kN in six steps. Time waves and frequency spectrums at all test runs are analyzed.

The time waves and frequency spectrums of acoustic emission for one test condition is shown in Figure 5. Similarly, remaining test runs were conducted with different defect sizes with various speeds and load conditions.

Fig .4. Test bearing

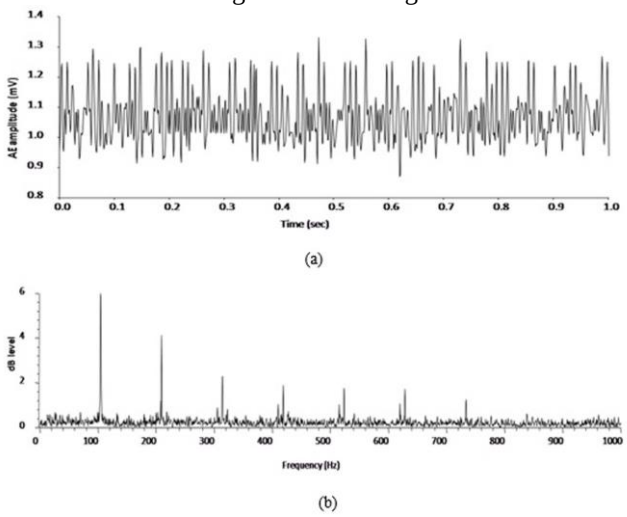

Fig. 5. AE (a) Time wave (b) Frequency spectrum of test conditions L2-D3-N6

4.1. ANOVA for AE amplitude (dB level)

Consisted AE amplitudes (dB level) at defect frequencies for defective bearing with different defects width D1-D5 at the outer race under 2 kN and 4 kN loads are recorded. Experimental results of AE amplitude for 20 experiments were presented in the Table 3. The AE amplitude data was analyzed to identify significant parameters using ANOVA. Figure 6(a) is a normal probability plot of residuals AE amplitude that indicates behavior of residuals. More than 95% of experimental data of residuals fell within 3sigma. 3D surface plots of AE amplitude (R1) against various combinations of parameters are shown in Figures 6(b)–(d). It shows that outer race defects and shaft speed has most significant impact on the AE amplitude response.

In this study, ANOVA was carried out at 95% of confidence level to analyse experimental data of AE amplitudes (dB level). ANOVA of AE amplitudes (dB level) was presented in the Table 4.

The model terms which are having p-value less than 0.05 are considered as significant (Fabricio et al., 2010).

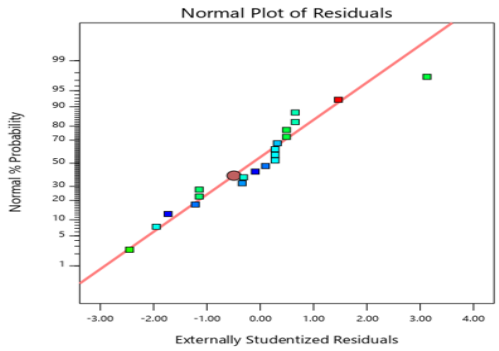

Fig. 6. (a). Normal probabilities of residuals for AE amplitude

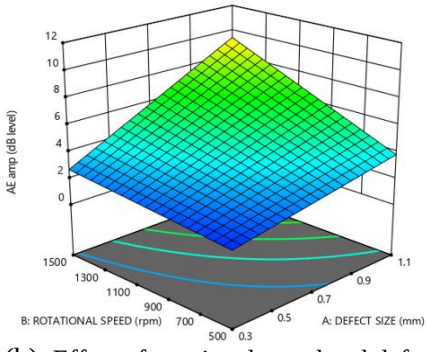

Fig. 6. (b). Effect of rotational speed and defect size on AE amplitude

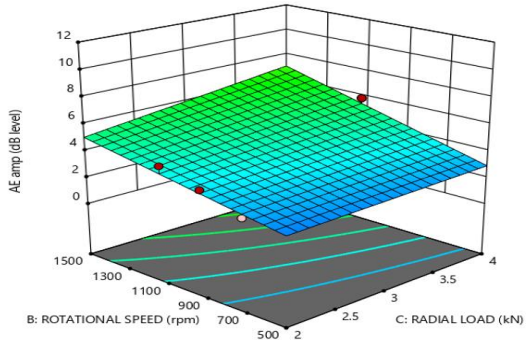

Fig. 6. (c). Effect of rotational speed and Radial load on AE amplitude

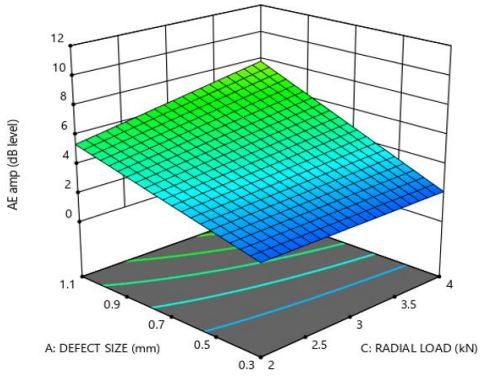

Fig. 6. (d). Effect of defect size and radial load on AE amplitude

In this section, the ANOVA model has p-value of 0.0001 that indicates that the model is significant. Helix angle, feed rate, spindle speed, interaction of helix angle and feed rate and another interaction of helix angle and spindle speed are having p-values 0.0001, 0.0001, 0.0223, 0.0184 and 0.0196 respectively. All the three parameters are to be found significant on the AE amplitudes (dB level). The R^2 value and adjusted R^2 value are equal to 0.9033 and 0.8587 respectively. The adequate precision value is equal to 18.9682, which is a ratio of signal to noise. A ratio greater than 4 is desirable (Bhardwaj et al., 2014). Empirical or regression equations for AE amplitudes (dB level) in terms of defect sizes, rotational speeds and radial loads were given below:

$$AEamp = +4.38 + 2.25A + 1.69B + 0.6118C + \quad (1)$$
$$+1.13AB + 0.6126AC + 0.3960BC$$

Table. 4. ANOVA for AE amplitude

Source	Sum of Squares	df	Mean Square	F-value	p-value
Model	94.33	6	15.72	20.25	0.0001
A-defect size (mm)	42.39	1	42.39	54.60	0.0001
B-rotational speed (rpm)	25.88	1	25.88	33.33	0.0001
C-radial load (kN)	6.93	1	6.94	8.93	0.0105
AB	10.22	1	10.22	13.17	0.0031
AC	3.14	1	3.14	4.05	0.0654
BC	1.43	1	1.43	1.84	0.1980
Residual	10.09	13	0.7764		
Cor Total	104.42	19			
Std. Dev	0.8811				
	R^2=0.9033				
Mean=4.41	Adjusted R^2=0.8587				
C.V.%=19.98	Predicted R^2 = 0.5416		Adeq precision=18.9682		

With the regression equation (1), the RSM had predicted the AE amplitudes (dB level). The predicted values for all trials were given in the Table 5. The RMS was performed using Design-Expert 11 software.

Table 5. Experimental and predicted values of AE amplitude (dB level).

Trail. No.	Design of experiments			AE amplitude (dB)	
	Defect size (mm)	Rotational speed (rpm)	Radial load (kN)	Exp	RSM
1	0.3	500	2	1.14	1.96
2	0.7	700	2	2.71	2.99
3	0.7	1100	2	4.58	4.02
4	1.1	1500	2	6.87	7.82
5	1.1	500	2	3.16	2.99
6	1.1	500	4	3.98	4.65
7	0.7	1100	4	5.83	5.41
8	0.3	1500	2	2.34	2.29
9	0.7	1100	4	5.83	5.41
10	0.3	500	4	1.13	1.17
11	0.7	900	2	3.75	3.51
12	0.7	900	2	3.75	3.51
13	0.7	900	2	3.75	3.51
14	0.7	1100	2	4.58	4.02
15	0.7	1300	4	5.31	6.24
16	0.7	1300	4	5.31	6.24
17	0.5	1300	4	4.21	4.47
18	0.5	1100	4	5.84	3.86
19	1.1	1500	4	11.8	11.06
20	0.3	1500	4	2.34	3.08

4.2. Optimised Results

The process optimization was done using RSM's D-optimal Test. The optimized value of input is shown in Figure 7. Desirability function is an important function in optimization to estimate acceptance of the optimized values (Adem et al., 2015). Desirability value of the optimization is calculated with a gradient algorithm between 0 and 1.

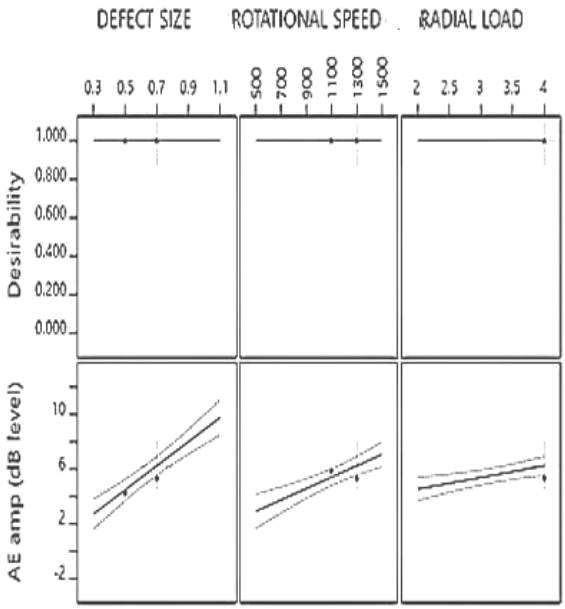

Fig.7. Optimization of AE amplitude

Optimization of process parameters was carried out for minimization of AE amplitude. Desirability values were found to be 1.0 for AE amplitude. The desirability value, 1 indicates to accept for optimization (Murath et al., 2014). Design expert software was used for optimization of operating parameters.

5. CONCLUSIONS

This experiment involves running the test-rig under specific speed and load with various sizes of seeded defects on test bearings, from which AE signals data were acquired. The following conclusions can be drawn from this investigation.

The defects were seeded in various sizes of width 0.3mm, 0.5mm, 0.7mm and 0.9 mm. Depth of defect 0.3mm were maintained in all test bearings. AE amplitudes (dB level) at defect frequencies for a defective bearing (0.5 mm width defect at outer race) under radial load are presented. Defect size of different sizes in the outer race results in vibration there after it produce amplitudes on time wave spectrum. ANOVA conforms that the mathematical models of AE amplitude were well fitted to experimental data. AE amp increases with increase of defect size and rotational speed but the effect of load on the AE amplitude found to be less.

With the regression equation, the RSM had predicted the AE amplitudes (dB level). Optimization of operating parameters was carried out for minimization of AE amplitude of the signals in dB level. Optimum key parameters were found as 1.1mm of defect size, 1300rpm of rotational speed and 4kN of radial load.

6. REFERENCES

1. Adem C., Turgay K., Ergun E. (2015). *Optimization of drilling parameters using Taguchi technique and response surface methodology (RSM) in drilling of AISI 304 steel with cryogenically treated HSS drills*. Journal of Intelligent Manufacturing, 26(2), 295–305.

2. Al-Obaidi S.M.A., Salman Leong M., Raja Hamzah R.I., Ahmed M. Abdelrhman, (2012). *A Review of Acoustic Emission Technique for Machinery Condition Monitoring: Defects Detection & Diagnostic*, Applied Mechanics and Materials, 229-231(1), 476-1480.

3. Bhuvnesh Bhardwaj, Rajesh Kumar, Pradeep K. Singh, (2014). *Surface roughness prediction model for turning of AISI 1019 steel using response surface methodology and Box-Cox transformation*, Proc. Inst. Mech. E Part B: J. Eng. Manuf., 228(2), 223–232.

4. Bouchra Abou El Anouar, (2017). *A comparative experimental study of different methods in detection and monitoring bearing defects*, International Journal of Advanced Scientific and Technical Research, 7(1), 409-423.
5. Caesarendra W. B., Kosasih A.K., Tieu H., Zhu C.A.S., Moodie Q. Zhu, (2016). *Acoustic emission-based condition monitoring methods: Review and application for low speed slew bearing*, Mechanical Systems and Signal Processing 72-73(1), 134–159.
6. Cockerill A., Clarke A., Pullin R., Bradshaw T. P., Cole, Holford K.M., (2016). *Determination of rolling element bearing condition via acoustic emission*, Proceedings of the Institution of Mechanical Engineers, Part J: Journal of Engineering Tribology, 230(11), 1377–1388.
7. Fabricio Jose Pontes, Messias Borges Silva, Joao Roberto Ferreira, Anderson Paulo de Paiva, Pedro Paulo Balestrassi, Gustavo Bonnard Schonhorst, (2010). *DOE Based Approach for the Design of RBF Artificial Neural Networks Applied to Prediction of Surface Roughness in AISI 52100 Hardened Steel Turning*", J. of the Braz. Soc. of Mech. Sci. & Eng., XXXII (5), 503.
8. Farzad Hemmati, Wasim Orfali, Mohamed S. Gadala, (2016). *Roller bearing acoustic signature extraction by wavelet packet transform, applications in fault detection and size estimation*, Applied Acoustics, 104, 101–118.
9. Gu D.S., Kim J.G., An Y.S., Choi B.K. (2011). *Detection of faults in gearboxes using acoustic emission signal*, Journal of Mechanical Science and Technology, 25(1), 1279-1286.
10. Jaeyoung Kim, (2017). *Incipient fault diagnosis in bearings under variable speed conditions using multiresolution analysis and a weighted committee machine*, J. Acoust. Soc. Am. 142(1), 35-41.
11. Jamadar, I. M, Vakharia, D.P., (2016). *An in-situ synthesized model for detection of defective roller in rolling bearings*, Engineering Science and Technology, 19(1), 1488–1496.
12. Ribeiro J. E., Cesar M. B., Pereira A. I., (2018). *The use of Response Surface Optimization Method to minimize the vibrations in the Milling Process*, Proceedings IRF2018: 6th International Conference Integrity-Reliability-Failure Lisbon/Portugal, 20(1), 1137-1144.
13. Ribeiro J., Lopes H., Queijo L., Figueiredo D. (2017), *Optimization of Cutting Parameters to Minimize the Surface Roughness in the End Milling Process Using the Taguchi Method*, Periodica Polytechnica Mechanical Engineering, 61(1), 30-35.
14. Kankar P.K., Satish C. Sharma, Harsha S.P., (2012). *Vibration signature analysis of a high-speed rotor supported on ball bearings due to localized defects*, Journal of Vibration and Control, 9(12), 1833–1853.
15. Ked Douche M., Thomas M., Tahan A., (2014). *Empirical Mode Decomposition of Acoustic Emission for Early Detection of Bearing Defect*s, Advances in Condition Monitoring of Machinery in Non-Stationary Operations, Springer, Berlin, 31(8), 367–377.
16. Sarıkaya M., Gullu A., (2014). *Taguchi design and response surface methodology-based analysis of machining parameters in CNC turning under MQL*, J. Clean. Prod., 65, 604–616.
17. Nerella M.J, Ratnam Ch., Rao V.V., (2017). *Study of Detection of Defects in Rolling Element Bearings Using Acoustic Measurement Methods - A Review*, SSRG International Journal of Mechanical Engineering (SSRG-IJME), 5, 110–116.
18. Rao V.V., Ratnam Ch., (2015). *A Comparative Experimental Study on Identification of Defect Severity in Rolling Element Bearings using Acoustic Emission and Vibration Analysis*, Tribology in Industry, 37(2), 176-185.
19. Tandon N., Choudhury A., (2000). *Application of acoustic emission technique for the detection of defects in rolling element bearings*. Tribology International, 33(1), 39–45.
20. Tandon N., Choudhury A. (1999). *A review of vibration and acoustic measurement methods for the detection of defects in rolling element bearings*, Tribology International, 32(1), 469-480.

Received: June 25, 2018 / Accepted: June 15, 2019 / Paper available online: June 20, 2019 © International Journal of Modern Manufacturing Technologies.